5 Density Functional Theories and Self-energy Approaches

Rex W. Godby[*] and Pablo García-González[†]

[*] Department of Physics, University of York,
Heslington, York YO10 5DD,
United Kingdom
`rwg3@york.ac.uk`

[†] Departamento de Física Fundamental,
Universidad Nacional de Educación
a Distancia, Apto. 60141, 28080 Madrid, Spain
`pgarcia@fisfun.uned.es`

Rex Godby

5.1 Introduction

One of the fundamental problems in condensed-matter physics and quantum chemistry is the theoretical study of electronic properties. This is essential to understand the behaviour of systems ranging from atoms, molecules, and nanostructures to complex materials. Since electrons are governed by the laws of quantum mechanics, the many-electron problem is, in principle, fully described by a Schrödinger equation (supposing the nuclei to be fixed). However, the electrostatic repulsion between the electrons makes its numerical resolution an impossible task in practice, even for a relatively small number of particles.

Fortunately, we seldom need the full solution of the Schrödinger equation. When one is interested in *structural* properties, the ground-state total energy of the system is sufficient. In other cases, we want to study how the system responds to some external probe, and then knowledge of a few excited-state properties must be added. For instance, in a direct photoemission experiment a photon impinges on the system and an electron is removed. In an inverse photoemission process, an electron is absorbed and a photon is ejected. In both cases we have to deal with the gain or loss of energy of the N electron system when a single electron is added or removed, i.e. with the one-particle spectra. If the electron is not removed after the absorption of the photon, the system had evolved from its ground-state to an excited state, and the process is described by a set of *electron-hole* excitation energies. These few examples reflect the fact that practical applications of quantum theory are actually based on more elaborated and specialised techniques than simply trying to solve directly the Schrödinger equation. As we may see in other chapters of this book, the ground-state energy can be obtained – in principle exactly – using density functional theory (DFT) [1,2]. Regarding excited

states, the information about single particle spectra is contained in the so called one-electron Green's function, whereas the electron-hole properties are described by the two-electron Green's function. Many-body perturbation theory (MBPT) [3,4,5,6,7], which focuses on these Green's functions directly, is a natural tool for the study of these phenomena.

Interestingly, the one-electron Green's function can also be used to calculate the ground-state energy as well as the expectation value of any one-particle observable (like the density or the kinetic energy) which is that DFT most naturally addresses[1]. This opens an appealing possibility: the use of MBPT instead of DFT in those cases in which the latter – because of the lack of knowledge of the *exact* exchange-correlation (xc) energy functional $E_{\mathrm{xc}}[n]$ – does not provide accurate results. For example, systems in which van der Waals bonds are important are completely outside the scope of the familiar local-density (LDA) or generalised gradient (GGA) approximations. However, we shall see that these van der Waals forces can be studied through MBPT within Hedin's GW approximation [8,4] which is the most widely used many-body method in solid-state physics.

In this chapter, after a brief introduction to MBPT and Hedin's GW approximation, we will summarise some peculiar aspects of the Kohn-Sham xc energy functional, showing that some of them can be illuminated using MBPT. Then, we will discuss how to obtain ground-state total energies from GW. Finally, we will present a way to combine techniques from many-body and density functional theories within a generalised version of Kohn-Sham (KS) DFT.

5.2   Many-Body Perturbation Theory

Our discussion focuses on the concepts from MBPT that will be useful in this chapter. We will also present a short overview of some current problems in *ab-initio* calculations of quasiparticle properties. We refer the reader to [3,4,5,6,7] and the review articles [9,10,11,12,13] for further information on theoretical foundations and applications to solid-state physics, respectively.

5.2.1   Green's Function and Self-energy Operator

Green's functions are the key ingredients in many-body theory from which relevant physical information can be extracted. Given a non-relativistic N electron system under an external potential $v_{\mathrm{ion}}(\boldsymbol{x})$, the one-particle Green's function (for simplicity we henceforth omit the prefix "one-particle") is defined as

$$G(\boldsymbol{x}, \boldsymbol{x}'; t - t') = -\mathrm{i} \left\langle \Psi_N^{(0)} \left| \mathcal{T} \left[\widehat{\psi}(\boldsymbol{x}, t) \, \widehat{\psi}^\dagger(\boldsymbol{x}', t') \right] \right| \Psi_N^{(0)} \right\rangle ; \qquad (5.1)$$

---

[1] Similarly, two-particle ground-state quantities, like the pair correlation function, can be obtained from the two-electron Green's function.

where $\boldsymbol{x} \equiv (\boldsymbol{r}, \xi)$ symbols the space and spin coordinates, $\left| \Psi_N^{(0)} \right\rangle$ is the ground-state of the system, $\widehat{\psi}(\boldsymbol{x}, t)$ is the annihilation operator in the Heisenberg picture, and $\mathcal{T}$ is Wick's time-ordering operator[2]. We may see that for $t > t'$, the Green's function is the probability amplitude to find an electron with spin ξ at point $\boldsymbol{r}$ and time t if the electron was added to the system with spin ξ' at point $\boldsymbol{r}'$ and time t'. When $t' > t$, the Green's function describes the propagation of a hole created at t.

As commented, the Green's function contains the information about one-particle excitations (we will see in Sect. 5.4 how to obtain ground-state properties). We start from the Lehmann representation of the Green's function:

$$G(\boldsymbol{x}, \boldsymbol{x}'; \omega) = \sum_n \frac{f_n(\boldsymbol{x}) f_n^*(\boldsymbol{x}')}{\omega - \mathcal{E}_n - \mathrm{i}\eta \, \mathrm{sgn}(\mu - \mathcal{E}_n)} \ . \tag{5.2}$$

Here, $G(\omega)$ is the Fourier transform with respect to $\tau = t - t'$, η is a positive infinitesimal, μ is the Fermi energy of the system, and

$$
\begin{aligned}
f_n(\boldsymbol{x}) &= \left\langle \Psi_N \left| \widehat{\psi}(\boldsymbol{x}) \right| \Psi_{N+1}^{(n)} \right\rangle \ , \ \mathcal{E}_n = E_{N+1}^{(n)} - E_N^{(0)} \ \text{if} \ \mathcal{E}_n > \mu \\
f_n(\boldsymbol{x}) &= \left\langle \Psi_{N-1}^{(n)} \left| \widehat{\psi}(\boldsymbol{x}) \right| \Psi_N \right\rangle \ , \ \mathcal{E}_n = E_N^{(0)} - E_{N-1}^{(n)} \ \text{if} \ \mathcal{E}_n < \mu
\end{aligned} \ , \tag{5.3}
$$

with $E_N^{(0)}$ the ground-state energy and $\left| \Psi_{N\pm 1}^{(n)} \right\rangle$ the n-th eigenstate with energy $E_{N\pm 1}^{(n)}$ of the $N \pm 1$ electron system. By taking the imaginary part of (5.2) we have the so-called spectral function:

$$A(\boldsymbol{x}, \boldsymbol{x}'; \omega) = \frac{1}{\pi} \left| \Im G(\boldsymbol{x}, \boldsymbol{x}'; \omega) \right| = \sum_n f_n(\boldsymbol{x}) f_n^*(\boldsymbol{x}') \delta(\omega - \mathcal{E}_n) \ . \tag{5.4}$$

We may see that $A(\boldsymbol{x}, \boldsymbol{x}'; \omega)$ is just the superposition of delta functions with weights given by the amplitudes $f_n(\boldsymbol{x})$ centred at each of the one-particle excitation energies $\mathcal{E}_n$. That is, as anticipated above, the Green's function reflects the one-particle excitation spectra. Moreover, such weights – see (5.3), depend on the density of available eigenstates after the addition/removal of one electron. Further details about the role of $A(\omega)$ in the interpretation of photoemission experiments can be found in [14].

The spectral function – actually selected diagonal matrix elements $A_{nn}(\omega)$ in a suitable one-electron basis representation – may exhibit well-defined structures reflecting the existence of highly probable one-electron excitations. Due to the Coulomb interaction, we cannot assign each excitation to an independent particle (electron or hole) added to the system with the excitation energy. Nonetheless, some of these structures can be explained *approximately* in terms of a particle-like behaviour, so having a *quasiparticle* (QP) peak. Where a second peak is required we may have what is called a *satellite*.

_____

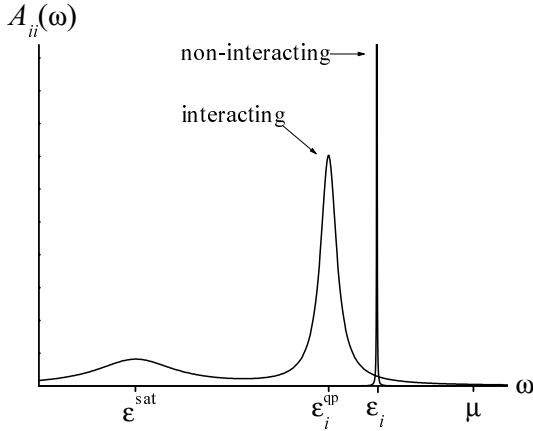[2] Note that G depends on $t - t'$ due to translational time invariance.

Fig. 5.1. Comparison between the non-interacting spectral function for a hole and the interacting one. Note how the interaction shifts down and broadens the QP peak and the appearance of a satellite at $\omega = \varepsilon^{\text{sat}}$

Of course this distinction is somewhat arbitrary, but a way of doing it is the following. Let us suppose that we switch off the interaction, so having a system of independent particles whose eigenstates can be described using one-electron orbitals $\phi_j(\boldsymbol{r})$ with eigenenergies ε_j. In this case, the matrix elements of the spectral function in the orbital basis set are

$$A_{ij}(\omega) = \langle \phi_i | A(\boldsymbol{x}, \boldsymbol{x}'; \omega) | \phi_j \rangle = \delta_{ij} \delta(\omega - \varepsilon_i)$$

That is, for the non-interacting system $A_{ii}(\omega)$ is just a delta function centred at $\omega = \varepsilon_i$ and the orbital energies are the one-electron excitation energies. If now we turn on the interaction, we may see that the delta function changes its position, broadens, and loses spectral weight which is transferred into the spectral background of the interacting $A_{ii}(\omega)$ – see Fig. 5.1. At the end of the process, the delta function has become a QP peak – in the sense that it originates from an independent single-particle state – and further structures that might have appeared would be the satellites. Note that the width of the QP peak reflects the finite lifetime of the added-particle state since it is not longer a real eigenstate of the system, whereas the satellites often reflect its resonant coupling with other elementary excitations like plasmons.

This one-electron picture can be formally introduced with the aid of the so-called self-energy operator Σ, which is defined through the Dyson equation

$$G^{-1}(\boldsymbol{x}, \boldsymbol{x}'; \omega) = G_{\text{H}}^{-1}(\boldsymbol{x}, \boldsymbol{x}'; \omega) - \Sigma(\boldsymbol{x}, \boldsymbol{x}'; \omega) \ . \tag{5.5}$$

Here, we have used the Hartree Green's function

$$G_{\text{H}}^{-1}(\boldsymbol{x}, \boldsymbol{x}'; \omega) = \delta(\boldsymbol{x} - \boldsymbol{x}')[\omega - h_0(\boldsymbol{x})] \ , \tag{5.6}$$

that corresponds to the non-interacting system in which $h_0 (\boldsymbol{x})$ is the one-electron Hamiltonian under the external potential $v_{\mathrm{ion}} (\boldsymbol{x})$ plus the classical Hartree potential $v_{\mathrm{H}} (\boldsymbol{r})$. Then, it is evident that the self-energy contains the many-body effects due to Pauli exchange and Coulomb correlation, and that sharp structures in $G (\omega)$ are related to small expectation values of the frequency-dependent operator $\omega - \widehat{h}_0 - \widehat{\Sigma} (\omega)$. Moreover, if we extend the ω-dependence of the self-energy to complex frequencies, such structures can be attributed to zeros of the operator $\omega - \widehat{h}_0 - \widehat{\Sigma} (\omega)$, that is, to solutions of the *non-Hermitian* eigenvalue problem

$$h_0 (\boldsymbol{x}) \phi_n^{\mathrm{qp}} (\boldsymbol{x}) + \int \mathrm{d}\boldsymbol{x}' \, \Sigma (\boldsymbol{x}, \boldsymbol{x}', E_n^{\mathrm{qp}}) \phi_n^{\mathrm{qp}} (\boldsymbol{x}') = E_n^{\mathrm{qp}} \phi_n^{\mathrm{qp}} (\boldsymbol{x}) \ , \qquad (5.7)$$

with complex energies E_n^{qp}. This is the *quasiparticle* equation, where Σ plays the role of an effective frequency-dependent and non-local potential. We may see that the self-energy has a certain resemblance with the DFT xc potential $v_{\mathrm{xc}} (\boldsymbol{x})$ but, of course, the two objects are not equivalent. We have to bear in mind that the local and static $v_{\mathrm{xc}} (\boldsymbol{x})$ is part of the potential of the fictitious KS non-interacting system, whereas the self-energy may be thought of as the potential felt by an added/removed electron to/from the interacting system.

Now, it is easy to see the correspondence between the QP peaks in the spectral function and the quasiparticle states ϕ_n^{qp}. If we expand $\Sigma_n (\omega) = \langle \phi_n^{\mathrm{qp}} | \Sigma (\omega) | \phi_n^{\mathrm{qp}} \rangle$ around $\omega = E_n^{\mathrm{qp}}$ we have that

$$G_n (\omega) = \langle \phi_n^{\mathrm{qp}} | G (\omega) | \phi_n^{\mathrm{qp}} \rangle \simeq \frac{Z_n}{\omega - (\varepsilon_n^{\mathrm{qp}} + \mathrm{i}\Gamma_n)} \ , \qquad (5.8)$$

with $\varepsilon_n^{\mathrm{qp}} = \Re E_n^{\mathrm{qp}}$, $\Gamma_n = \Im E_n^{\mathrm{qp}}$, and Z_n the complex QP renormalisation factor given by

$$Z_n^{-1} = 1 - \left. \frac{\partial \Sigma_n (\omega)}{\partial \omega} \right|_{\omega = E_n^{\mathrm{qp}}} . \qquad (5.9)$$

As a consequence, if Γ_n is small, the spectral function $\Im G_n (\omega)$ is expected to have a well defined peak centred at $\varepsilon_n^{\mathrm{qp}}$ of width Γ_n and weight $|\Re Z_n|$. Therefore, the real part $\varepsilon_n^{\mathrm{qp}}$ is the QP energy itself, and it provides the band-structure of the system. The inverse of the imaginary part Γ_n^{-1} gives the corresponding QP lifetime.

5.2.2   Many-Body Perturbation Theory and the *GW* Approximation

In practical applications, we have to obtain (under certain unavoidable approximations) the self-energy operator. From this we calculate the QP spectrum using (5.7) and, if required, the full Green's function given by (5.5). MBPT provides a tool for such a task but, as in any other perturbation theory, we have to define the unperturbed system and the perturbation itself. In the

above discussion, the unperturbed system seemed to be the non-interacting system of electrons under the potential $v_{\text{ion}}(\boldsymbol{x}) + v_{\text{H}}(\boldsymbol{r})$. However, due to the obvious problems that arise when trying to converge a perturbation series, it is much better to start from a different non-interacting scenario, like the LDA or GGA KS system, which already includes an attempt to describe exchange and correlation in the actual system. Considering the perturbation, the bare Coulomb potential w is very strong and, besides, we know that in a many-electron system the Coulomb interaction between two electrons is readily screened by a dynamic rearrangement of the other electrons [15], reducing its strength. Therefore, it is much more natural to describe the Coulomb interaction in terms of a *screened* Coulomb potential W and then write down the self-energy as a perturbation series in terms of W. If we just keep the first term of such an expansion, we will have the GW approximation.

The self-energy can be obtained from a self-consistent set of Dyson-like equations known as Hedin's equations:

$$P(1\,2) = -\mathrm{i}\int \mathrm{d}(3\,4)\, G(1\,3)\, G(4\,1^+)\, \Gamma(3\,4,2) \tag{5.10a}$$

$$W(1\,2) = w(1\,2) + \int \mathrm{d}(3\,4)\, W(1\,3)\, P(3\,4)\, w(4\,2) \tag{5.10b}$$

$$\Sigma(1\,2) = \mathrm{i}\int \mathrm{d}(3\,4)\, G(1\,4^+)\, W(1\,3)\, \Gamma(4\,2,3) \tag{5.10c}$$

$$G(1\,2) = G_{\text{KS}}(1\,2) \tag{5.10d}$$
$$+ \int \mathrm{d}(3\,4)\, G_{\text{KS}}(1\,3)\, [\Sigma(3\,4) - \delta(3\,4)\, v_{\text{xc}}(4)]\, G(4\,2)$$

$$\Gamma(1\,2,3) = \delta(1\,2)\,\delta(1\,3) \tag{5.10e}$$
$$+ \int \mathrm{d}(4\,5\,6\,7)\, \frac{\delta\Sigma(1\,2)}{\delta G(4\,5)} G(4\,6)\, G(7\,5)\, \Gamma(6\,7,3) \ ,$$

where we have used the simplified notation $1 \equiv (\boldsymbol{x}_1, t_1)$ etc. Above, P is the irreducible polarisation, Γ is the so-called vertex function, and

$$G_{\text{KS}}(\boldsymbol{x}, \boldsymbol{x}'; \omega) = \sum_n \frac{\phi_n(\boldsymbol{x})\, \phi_n^*(\boldsymbol{x}')}{\omega - \varepsilon_n^{\text{KS}} - \mathrm{i}\eta\, \mathrm{sgn}(\mu - \varepsilon_n^{\text{KS}})} \ , \tag{5.11}$$

with G_{KS} the Green's function of the KS system and ϕ_n the corresponding KS wavefunctions with eigenenergies $\varepsilon_n^{\text{KS}}$. We arrive at the GW approximation by eliminating the second term in the vertex function (5.10e) (i.e. neglecting "vertex corrections") in such a way that (5.10a) and (5.10b) reduces to

$$P(1\,2) = -\mathrm{i} G(1\,2)\, G(2\,1^+) \tag{5.12a}$$
$$\Sigma(1\,2) = \mathrm{i} G(1\,2^+)\, W(1\,2) \ . \tag{5.12b}$$

That is, in GW the screened Coulomb potential is calculated at the RPA level and Σ is just the direct product of G and W (hence the name). Also note
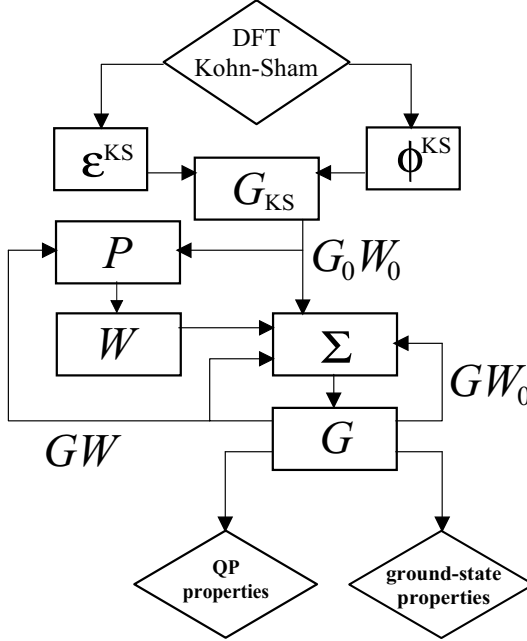
Fig. 5.2. Flow diagram sketching the practical implementation of the GW method. The partially self-consistent GW_0 updates the self-energy operator Σ, whereas the fully self-consistent GW also updates the screened Coulomb potential W

that in the Hartree-Fock approximation the Fock operator Σ_{x} is obtained as in (5.12b) but with W replaced by the static bare Coulomb potential w. Based on this, GW may be understood as a physically motivated generalisation of the Hartree-Fock method in which the Coulomb interaction is dynamically screened. A flow diagram sketching the practical implementation of the GW method is shown in Fig. 5.2.

In most GW applications, self-consistency is set aside, and P and Σ are obtained by setting $G = G_{\mathrm{KS}}$ in (5.12a) and (5.12b). The interacting Green's function is then obtained by solving (5.10e) once. Furthermore, in many cases there is an almost complete overlap between the QP and the KS wavefunctions, and the full resolution of the QP equation (5.7) may be circumvented. Thus, E_n^{qp} is given as a first-order perturbation of the KS energy $\varepsilon_n^{\mathrm{KS}}$:

$$E_n^{\mathrm{qp}} \simeq \varepsilon_n^{\mathrm{KS}} + \left\langle \phi_n \left| \Sigma \left(\varepsilon_n^{\mathrm{KS}} \right) - v_{\mathrm{xc}} - \Delta\mu \right| \phi_n \right\rangle \ , \qquad (5.13)$$

where a constant $\Delta\mu$ has been added to align the chemical potential before (KS level) and after the inclusion of the GW correction. As long as we are just interested on band-structures, further approximations, generally through a *plasmon-pole* ansatz [16], may be used to evaluate W in real materials. However, these models prevent us from calculating the whole Green's function

so losing important spectral features like QP lifetimes and they can hardly be justified in systems others than *sp* metals. An efficient procedure to find out the entire spectral representation of the self-energy is the so-called *space-time* method [17], in which dynamical dependencies are represented in terms of imaginary times and frequencies, and each of Hedin's GW equations is solved in the most favourable spatial representation. As a final step, the self-energy for real frequencies can be obtained using analytical continuation from its values at imaginary frequencies after a fitting to a suitable analytical function. This method shows a favourable scaling with system size and avoids fine ω-grids that were needed to represent sharp spectral features in $G_{\mathrm{KS}}(\omega)$ and $W(\omega)$ [17,18].

Since the first *ab-initio* calculations performed by Hybertsen and Louie in 1985 [19], non-self-consistent GW has been applied to calculate QP properties (band-structures and lifetimes) of a wide variety of systems. The most striking success of this "G_0W_0" approximation is the fairly good reproduction (to within $0.1\,\mathrm{eV}$ of experiments) of experimental band gaps for many semiconductors and insulators, so circumventing the well-known failure of LDA when calculating excitation gaps. It is also worth emphasising that G_0W_0 gives much better ionisation energies than LDA in localised systems [20,21,22], and its success when studying lifetimes of hot electrons in metals and image states at surfaces (see [11,12] and references therein).

In spite of its overall success, G_0W_0 has some limitations. For instance, agreement with experiment for energy gaps and transitions may mask an overall additive error in the value of the self-energy; satellite structures are not well described in detail; and agreement with experiment worsens away from the Fermi energy (notably the bandwidth of alkali metals). Further approximations not related to MBPT, like the use of pseudopotentials in practical *ab-initio*calculations and those simplifications made when interpreting experimental results have been also considered. The main conclusions can be summarised as follows:

- Inclusion of vertex corrections improves the description of the absolute position of QP energies in semiconductors [23] and the homogeneous electron gas (HEG) [24], although the amount of such corrections depends very sensitively on the model used for the vertex [25]. Vertex corrections constructed using the so-called cumulant expansion [26], reproduce the multiple-plasmon satellite structure in alkali metals [27] (the GW spectral function only shows an isolated satellite).
- On the other hand, the absence of vertex corrections does not seem to be the full explanation of the differences (0.3–$0.4\,\mathrm{eV}$) between the measured valence bandwidth for alkali metals [28,29] and the G_0W_0 values [30,31]. The inclusion of vertex effects slightly changes the occupied bandwidth of the HEG, but this correction is not enough to fit the experimental results [24,32,33]. Of course these results are not conclusive because any effect due to the crystal structure is neglected. Nonetheless, the fact that G_0W_0

plus vertex barely changes the valence bandwidth of Si [23], gives further indirect support to the existence of other mechanisms explaining this discrepancy. It seems plausible that specific details of the photoemission process could be the ultimate reason of the discrepancies between theory and experiment [9,33,34,35].

- The "bandwidth problem" mentioned above was the primary motivation of the first complete study of the role of self-consistency in GW performed by von Barth and Holm for the HEG [36,37]. Partially self-consistent "GW_0" calculations – in which W is calculated only once using the RPA, so that (5.12a) is not included in the iterative process – slightly *increase* the G_0W_0 occupied bandwidth. Results are even worse at full self-consistency in which, besides, there is not any well-defined plasmon structure in W and, as a consequence, the plasmon satellite in the spectral function practically vanishes. These results were confirmed by Schöne and Eguiluz [31] for bulk K where they obtained that the GW bandwidth is 0.6 eV broader than that of G_0W_0. These authors found another important result: self-consistency overestimates by 0.7 eV the experimental fundamental gap of Si, which is an error (but of the opposite sign) comparable with the one given by LDA. As a consequence, it does not seem a good idea to perform self-consistent GW calculations to obtain QP properties. The effects resulting from an unphysical screened Coulomb potential must be necessarily balanced by the proper inclusion of vertex corrections along the self-consistent procedure. However, as we will see in Sect. 5.4, such a self-consistency is essential to evaluate absolute ground-state energies.

- Very recently, a fully self-consistent calculation including vertex corrections has been reported for the HEG by Takada [35]. Compared with a G_0W_0 calculation (see Fig. 5.3), both methods give practically the same bandwidth, although the QP peak is much broader than in G_0W_0. The latter reflects a more effective damping of the QP due to the multiple electron-hole excitations that are included in diagrams beyond GW. A similar broadening can be observed in the first plasmon satellite peak, which it is fairly well located at the expected position (ω_p below the QP peak, ω_p being the bulk plasmon frequency). Interestingly, there is no significant change in the width of the valence band, but excellent agreement is obtained by including the self-energy corrections for the final state of the photoemitted electron. However, application of this self-consistent procedure to inhomogeneous systems appears to be very challenging.

- Finally, core electrons, that are absent from routine pseudopotential (PP) calculations, could be important in the final determination of spectral properties. Nonetheless, the inclusion of core-electrons in *ab-initio* MBPT schemes should be done with caution. For instance, an all-electron G_0W_0 calculation reduces the corresponding PP value of the fundamental gap of bulk Si at least 0.3 eV [38,39,40]. This effect has been interpreted as a result of exchange coupling between core and valence electrons [40] which, of course, is described in a PP calculation only at the level of the underlying
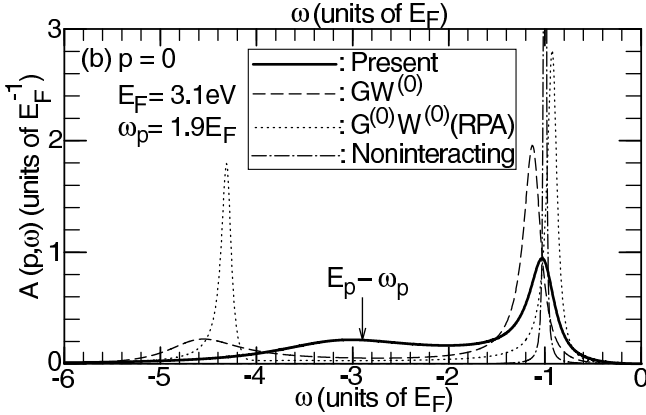
Fig. 5.3. Spectral function at the bottom of the valence band of the HEG ($r_s = 4$) given by a non-interacting picture, G_0W_0, GW_0, and a full self-consistent procedure with the inclusion of vertex corrections. After Takada [35]

atomic LDA calculation. However, the occupied bandwidth only suffers a marginal change of $0.1\,\text{eV}$ after an all-electron calculation (note that the experimental value is $12.5\,\text{eV}$). This might suggest that vertex corrections, that are almost irrelevant when determining the band gap of *sp* semiconductors under the PP approximation [23,41], could be more important in those situations in which valence states coexist with more localised core states. Furthermore, the performance of G_0W_0 in transition metals, with the corresponding appearance of more localised *d* states, has not been fully assessed yet [9]. For these reasons, the striking coincidence between the experimental Si band gap and the all-electron self-consistent *GW* result reported by Ku and Eguiluz [40] might be fortuitous.

In summary, G_0W_0 is an excellent approximation for the evaluation of QP properties of simple systems and, very likely, able to provide the main trends in more complex systems. Theories beyond G_0W_0 are required to study other spectral features.

5.3 Pathologies of the Kohn–Sham xc Functional

The Kohn-Sham formalism [2] relies on the link between an actual N electron system and a fictitious non-interacting counterpart through the xc potential $v_{\text{xc}}(\boldsymbol{r}) = \delta E_{\text{xc}}[n]/\delta n(\boldsymbol{r})^3$. Hence, $v_{\text{xc}}(\boldsymbol{r})$ contains essential information about many-body correlations which, as we have seen in the previous section, MBPT describes in terms of non-local dynamical functions. Then, we

---

^{3} For simplicity, in v_{xc} we omit the explicit functional dependence on the density.

can easily realise that the mapping between ground-state densities and KS potentials,

$$n\left(\boldsymbol{r}\right) \to v_{\mathrm{KS}}\left[n\right]\left(\boldsymbol{r}\right) = v_{\mathrm{ion}}\left(\boldsymbol{r}\right) + \int \mathrm{d}\boldsymbol{r}' \, \frac{n\left(\boldsymbol{r}'\right)}{\left|\boldsymbol{r} - \boldsymbol{r}'\right|} + v_{\mathrm{xc}}\left(\boldsymbol{r}\right) \ , \qquad (5.14)$$

must depend on $n\left(\boldsymbol{r}\right)$ in a very peculiar and sensitive way. In fact, the actual functional relation between $n\left(\boldsymbol{r}\right)$ and $v_{\mathrm{xc}}\left(\boldsymbol{r}\right)$ (or $E_{\mathrm{xc}}\left[n\right]$) is:

- highly non-analytical: small or even infinitesimal changes in the density may induce substantial variations of the xc potential;
- highly non-local[4]: changes in the density at a given point $\boldsymbol{r}$ may induce substantial variations of the xc potential at a very distant point $\boldsymbol{r}'$.

These conditions are the origin of some special features that we will review in this section, and show how difficult is to construct a fully reliable approximation to the exact xc energy or potential that is an explicit functional of the density. Note that the LDA does not fulfil either requirement, and GGAs are just analytical semi-local approaches. The novel meta-GGAs (see the chapter by John P. Perdew in this book) are interesting in the sense that they include further non-analytical and non-local behaviour through the explicit appearance of the KS wavefunctions. Their performance remains to be explored, but it is likely that some non-analyticities and non-locality of the exact functional remains beyond their grasp. In fact, the virtue of these models is their ability to provide accurate results in many situations being, at the same time, very easy to apply. Other alternatives, like averaged and weighted density approximations [42,43,44], are truly non-local prescriptions but, despite its complexity, are once more limited by their explicit dependence on the density. Finally, we would like to mention the existence – as discussed by E. Engel in this book – of a very promising *third generation* of xc energy density functionals. In these models, the exchange energy – which is already non-local and non-analytical – is treated exactly [45,46], and then only Coulomb correlations remains to be approximated. The only drawback is that they do not benefit any more from the well-known cancellation between exchange and correlation effects in extended systems which, somehow, is exploited by other approximations. Therefore, the correlation part should be, in principle, more sophisticated than an LDA or GGA. To what extent these new functionals incorporate the following peculiarities of the xc functional remains to be investigated.

---

[4] The non-local *density*-dependence of the xc potential should not be confused with whether the $v_{\mathrm{xc}}\left(\boldsymbol{r}\right)$ is a local or non-local potential in its dependence on its spatial argument $\boldsymbol{r}$; in Kohn-Sham theory the xc potential is always a *local* potential in the latter sense.

5.3.1   The Band Gap Problem

We have already mentioned the inaccuracy of LDA-KS when determining the band gap of semiconductors and insulators. This failure is intimately related to a pathological non-analytical behaviour of the xc energy functional, as shown by J. P. Perdew and M. Levy and by L. J. Sham and M. Schlüter [47,48]. Namely, the xc potential may be increased by a finite constant of the order of 1 eV as a result of the addition of an extra electron to an extended system, that is, after an infinitesimal change of the electron density.

   As is well known [49,50], the band gap E_{gap} of an N electron system is defined as the difference between the electron affinity $A = E_N^{(0)} - E_{N+1}^{(0)} \equiv -\mathcal{E}_{\text{LUMO}}$ and the ionisation potential $I = E_{N-1}^{(0)} - E_N^{(0)} \equiv -\mathcal{E}_{\text{HOMO}}$:

$$E_{\text{gap}} = I - A = \mathcal{E}_{\text{LUMO}} - \mathcal{E}_{\text{HOMO}} , \tag{5.15}$$

where HOMO and LUMO stand for highest occupied and lowest unoccupied molecular orbital respectively. We may see that the band gap (or the HOMO-LUMO gap in a finite system) is just the difference between two single-electron removal/addition energies, so it is immediately addressed by MBPT. We can also calculate E_{gap} using KS-DFT through the expression

$$E_{\text{gap}} = \varepsilon_{N+1}^{\text{KS}} (N + 1) - \varepsilon_N^{\text{KS}} , \tag{5.16}$$

where $\varepsilon_{N+1}^{\text{KS}} (N + 1)$ is the energy of the highest occupied KS orbital of the $N + 1$ electron system, and $\varepsilon_N^{\text{KS}}$ is the HOMO level of the KS N-particle system – note that we keep the notation introduced in the previous section, in which $\varepsilon_i^{\text{KS}}$ is the i-th KS orbital energy of the N electron system. It is easy to arrive at (5.16) just bearing in mind that the affinity of an N electron system is the opposite of the ionisation potential of the $N + 1$ electrons, and that the Kohn-Sham HOMO level equals the actual one[5] [51].

   For a non-interacting system, the gap can be readily written in terms of its orbital energies. Therefore, for the fictitious N electron KS system we have

$$E_{\text{gap}}^{\text{KS}} = \varepsilon_{N+1}^{\text{KS}} - \varepsilon_N^{\text{KS}} . \tag{5.17}$$

From (5.16) and (5.17), we immediately get that the actual and KS gaps are related through

$$E_{\text{gap}} = \left(\varepsilon_{N+1}^{\text{KS}} - \varepsilon_N^{\text{KS}} \right) + \left(\varepsilon_{N+1}^{\text{KS}} (N + 1) - \varepsilon_{N+1}^{\text{KS}} \right) \equiv E_{\text{gap}}^{\text{KS}} + \Delta_{\text{xc}} , \tag{5.18}$$

an expression which is illustrated in Fig. 5.4. We may see that Δ_{xc} is just the difference between the energies of the $(N + 1)$-th orbitals of the KS systems that correspond to the neutral and ionised electron systems. In a solid, in which $N \gg 0$, the addition of an extra electron only induces an infinitesimal

---

[5] That is, for an N electron system $\varepsilon_N^{\text{KS}} = -I$. Remember that this is the only KS orbital energy with an explicit physical meaning.
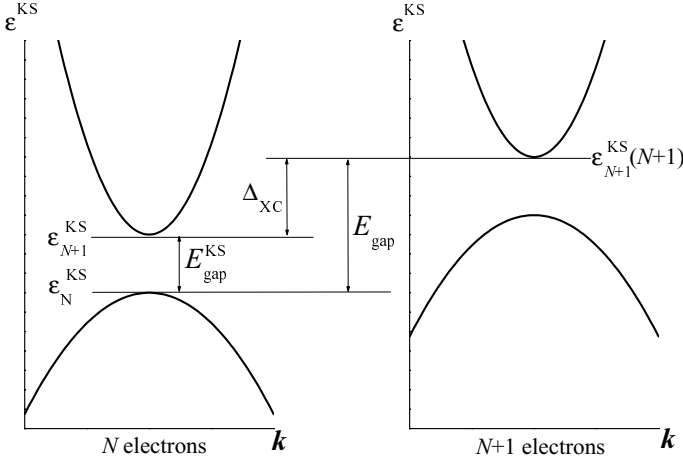
Fig. 5.4. Sketch of the Kohn-Sham band structure of a semiconductor (left panel). After the addition of an electron which occupies the empty conduction band, (right panel) the xc potential and the whole band-structure shift up a quantity Δ_{xc}

change of the density. Therefore, the two corresponding KS potentials must be practically the same inside the solid up to a constant shift and, consequently, the KS wavefunctions do not change. The energy difference Δ_{xc} is then the aforementioned rigid shift which, in addition, is entirely contained in v_{xc} because the Hartree potential depends explicitly on the density. As a conclusion, Δ_{xc} is the measure of a well-defined non-analytical behaviour of the xc energy functional. Namely, it is a finite variation of $v_{\mathrm{xc}}(\boldsymbol{r})$ extended everywhere in the solid due to an infinitesimal variation of $n(\boldsymbol{r})$

$$\Delta_{\mathrm{xc}} = \left(\left. \frac{\delta E_{\mathrm{xc}}[n]}{\delta n(\boldsymbol{r})} \right|_{N+1} - \left. \frac{\delta E_{\mathrm{xc}}[n]}{\delta n(\boldsymbol{r})} \right|_{N} \right) + \mathcal{O}\left(\frac{1}{N} \right) . \qquad (5.19)$$

Now it is easy to see the relation between a non-analytical v_{xc} and the band gap problem. If v_{xc} were actually discontinuous, the actual band gap would not be given in terms of the KS energies of the N electron system[6]. On the contrary, if Δ_{xc} were zero (or very close to zero), the difference between the actual gap and the LDA-KS one $E_{\mathrm{gap}}^{\mathrm{LDA}}$ would be just an inherent limitation of the local-density approximation. In the latter case, the formulation of more sophisticated approaches to the xc energy would allows us to calculate the gap of a real material directly from its corresponding KS band-structure. Nonetheless, the LDA is already a good approximation when calculating total energies and densities of bulk semiconductors and, moreover, improvements upon the LDA, such as the GGA or the WDA, change the KS gap very little.

---

[6] In a similar context this is what happens in a metal. Although the KS Fermi energy is equal to the actual one, the corresponding Fermi surfaces may differ.

Table 5.1. The xc discontinuity Δ_{xc}, and calculated and experimental fundamental band gaps, for four semiconductor and insulators. All energies are in eV. From Godby *et al.* [53]

	Si	GaAs	AlAs	Diamond
Δ_{xc}	0.58	0.67	0.65	1.12
Band gaps:				
KS-LDA	0.52	0.67	1.37	3.90
G_0W_0	1.24	1.58	2.18	5.33
Experiment	1.17	1.63	2.32	5.48

The existence of a discontinuity in v_{xc} is, then, more plausible than an error in the LDA band-structure.

The first evidence of a non-zero Δ_{xc} in real matter was given by Godby *et al.* [52,53] who used the so-called Sham-Schlüter equation [48,54],

$$\int \mathrm{d}\boldsymbol{r}'\, v_{\mathrm{xc}}\left(\boldsymbol{r}'\right) \int \mathrm{d}\omega\, G_{\mathrm{KS}}\left(\boldsymbol{r}, \boldsymbol{r}'; \omega\right) G\left(\boldsymbol{r}', \boldsymbol{r}; \omega\right)$$

$$= \int \mathrm{d}\boldsymbol{r}'\, \mathrm{d}\boldsymbol{r}'' \int \mathrm{d}\omega\, G_{\mathrm{KS}}\left(\boldsymbol{r}, \boldsymbol{r}''; \omega\right) \Sigma\left(\boldsymbol{r}', \boldsymbol{r}''; \omega\right) G\left(\boldsymbol{r}'', \boldsymbol{r}; \omega\right) , \qquad (5.20)$$

to calculate the xc potential from the many-body self-energy operator, which was obtained under the *GW* approximation. This MBPT-based potential was found to be very similar to the LDA one and the corresponding band structures turned out to be practically the same. As a consequence, the xc discontinuity Δ_{xc} is the main cause of the difference between the experimental gaps and those given by the LDA. In fact, Δ_{xc} accounts for about 80% of the LDA band gap error for typical semiconductors and insulators (see Table 5.1). This result was confirmed by Knorr and Godby for a family of model semiconductors [55]. In this case, the exact potential $v_{\mathrm{KS}}\left(\boldsymbol{r}\right)$ (and hence, the exact $E_{\mathrm{gap}}^{\mathrm{KS}}$) was calculated by imposing the reproduction of quantum Monte-Carlo densities. Again $\Delta_{\mathrm{xc}} = E_{\mathrm{gap}}^{\mathrm{KS}} - E_{\mathrm{gap}} \neq 0$, accounting for 80% of the LDA error $E_{\mathrm{gap}} - E_{\mathrm{gap}}^{\mathrm{LDA}}$. Interestingly, an opposite trend (i.e. $\Delta_{\mathrm{xc}} \simeq 0$) was found by Gunnarsson and Schönhammer in a very different scenario: a simple Hubbard-like one-dimensional semiconductor in which v_{xc} and the gap can be obtained exactly [56].

Recently, Städele and co-workers [57] calculated the fundamental band gaps for a number of standard semiconductors and insulators using the exact exchange functional together with the local approximation to the correlation energy (which we denote EXX(c)). In several of the materials studied the KS gaps within this approximation were found to be notably closer to experiment than the LDA gaps. However, the same paper also evaluated the exchange contribution to Δ_{xc} (defined as the difference between the Hartree-Fock and exact-exchange KS gaps [59]), which was several electron volts, much larger
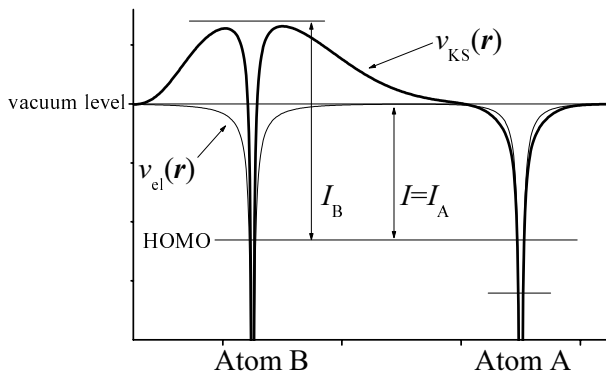
Fig. 5.5. The Kohn-Sham effective potential $v_{KS}(\boldsymbol{r})$ for two widely separated open shell atoms. Whereas the classical contributions to v_{KS} do not show any pathological behaviour, the exchange-correlation potential takes a positive value $I_B - I_A$ around the atom B

than any estimate of the total Δ_{xc}. This serves to emphasise the large degree of cancellation between exchange and correlation effects, familiar from other aspects of the electronic structure of solids, which suggests that caution must be exercised in interpreting a calculation in which exchange and correlation are treated on quite different footings. In a further paper [58], G_0W_0 band gaps calculated from EXX(c) wavefunctions were found to be little different from those calculated from LDA wavefunctions, supporting the notion that a variety of reasonable descriptions of exchange and correlation provide adequate zeroth-order starting points for a MBPT calculation.

5.3.2   Widely Separated Open Shell Atoms

It is known that the xc potential is, in many cases, long ranged. For instance, in a neutral atom $v_{xc}(\boldsymbol{r})$ decays asymptotically as $-1/r$, whereas for a metal surface it exhibits an image-like behaviour $-1/4z$ [51]. What it is not so known is that, as shown by Almbladh and von Barth [60], under some special circumstances, $v_{xc}(\boldsymbol{r})$ can be macroscopically long-ranged, thus reflecting a pathological *ultra-high* non-locality.

Let us consider two atoms A and B, each of them with an unpaired electron, whose ionisation potentials are I_A and I_B with $I_A < I_B$. If the atoms are separated by a very large arbitrary distance d, the ionisation potential of the whole system I is then given by the smallest (I_A) of the two ionisation potentials. Taken into account that in a finite system the ground-state density decays as $n(\boldsymbol{r}) \propto \exp\left(-2r\sqrt{2I}\right)$ [51,61], the asymptotic behaviour of the ground-state density of this "molecule" is governed by $I = I_A$ except in a region surrounding atom B, where the exponential fall-off of the density is given in terms of I_B.

If the ground-state of the N-particle system is a spin singlet[7], the highest occupied state ϕ_N of the KS fictitious system with energy $\varepsilon_N^{\mathrm{KS}} = -I = -I_{\mathrm{A}}$ is doubly occupied – remember that all the lower KS-states must be completely full. All the asymptotic behaviour of the density is determined by the HOMO, thus there is a region around the atom B in which $v_{\mathrm{KS}} - \varepsilon_N^{\mathrm{KS}} \simeq I_{\mathrm{B}}$ whereas $v_{\mathrm{KS}} - \varepsilon_N^{\mathrm{KS}}$ tends to I_{A} in the rest of the system – see Fig. 5.5. Both electrostatic and ionic contributions to v_{KS} decay to zero everywhere. Therefore, although the xc potential decays to zero around the atom A and, in general, at sufficiently large distances, v_{xc} tends to $I_{\mathrm{B}} - I_{\mathrm{A}} > 0$ in the neighbourhood of the atom B. That is, v_{xc} shifts up a finite amount around B due to the presence of another electron at an arbitrary large distance. Moreover, v_{xc} must have a spatial variation in a region between A and B where the electron density is practically zero. Both features clearly illustrate that the xc potential exhibits an unphysical infinite range in this model system. Note that this behaviour cannot emerge by any means from typical non-local prescriptions which assume a finite range around a point $\boldsymbol{r}$ that depends on the density $n(\boldsymbol{r})$.

5.3.3   The Exchange-Correlation Electric Field

An insulating solid is, of course, composed of individual unit cells, each of which contains polarisable electrons which may become slightly displaced in response to an applied uniform electric field, so that each unit cell acquires an electric dipole moment. According to the well-known theory of dielectric polarisation, this *macroscopic polarisation* produces a "depolarising" electrostatic field which reduces the net electric field by a factor of ε, the macroscopic dielectric constant. In Kohn-Sham DFT, however, there is a further possible contribution to the potential felt by the Kohn-Sham electrons: the exchange-correlation potential $v_{\mathrm{xc}}(\boldsymbol{r})$ may also acquire a long-range variation, which was termed the exchange-correlation "electric field" by Godby and Sham, and Gonze, Ghosez and Godby in a series of papers [62,63,64,65,66,67]. (Of course, it is not truly an *electric* field in the sense that it is produced by real electric charge, but its effect on the Kohn-Sham potential is the same as that of an electric field.)

Figure 5.6 shows the basic concept. The two polarised insulators shown in the central and lower parts of the Figure have identical electron densities, but different Kohn-Sham potentials: the two systems differ in their macroscopic polarisation. In order to reproduce the correct macroscopic polarisation, the exact Kohn-Sham xc potential must acquire a part which varies linearly in space: the xc field.

For our purpose, the point is that the exchange-correlation electric field is another pathological aspect of the exact Kohn-Sham xc functional: the

---

[7] If the ground-state were a triplet we should use the extension of KS-DFT to spin polarised systems, but in this case the pathology we are describing will not appear.
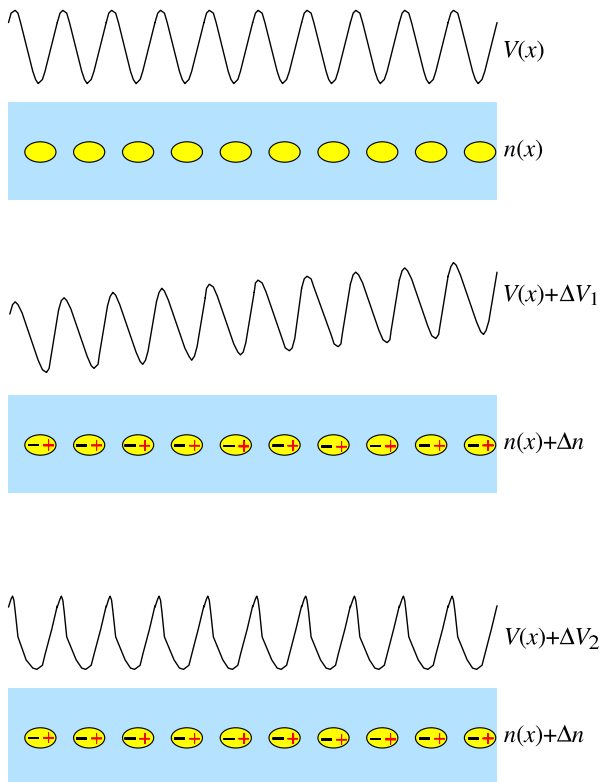
Fig. 5.6. A schematic illustration of the origin of the exchange-correlation "electric field". Top: an unpolarised insulator; the blobs represent the regions of high electron density within each unit cell. Centre: The same insulator, polarised by the addition of an external electric field, which (together with the depolarising internal electric field and any exchange-correlation "electric field") results in the total Kohn-Sham potential shown. Bottom: The same polarised electron density in the bulk crystal may be generated by a Kohn-Sham potential with zero net long-range field (as shown here), or indeed by a family of potentials, each with a different net field. Each member of the family corresponds to a different macroscopic polarisation, i.e. a different surface charge. A particular non-zero value of the Kohn-Sham exchange-correlation "electric field" is required to reproduce the correct macroscopic polarisation

electron density in the polarised insulator is the same from one unit cell to the next, while $v_{\mathrm{xc}}(\boldsymbol{r})$ rises by a constant amount over the same distance. Therefore, the xc potential cannot be regarded as a functional of the electron density within its own unit cell, or indeed the electron density in any finite region. The xc-field part of the potential depends on the polarisation; that is, on the electron density at the surface of the crystal. For this reason, the xc field represents an *ultra-non-local* dependence of the xc potential on the

electron density. In contrast, in a MBPT description, the self-energy operator, which is written as a perturbation series in terms of fairly local[8] quantities, is believed to have no such long-range variation from one cell to the next, and hence no "electric field". Thus, in a MBPT description, the long-range part of the effective potential is simply the external potential plus the actual electrostatic depolarising field.

A simple argument [63] indicates why the xc-field must be non-zero, and allows an estimate of its magnitude. Consider an unpolarised insulator, in which the band gap discontinuity is Δ_{xc}. Let us, for a moment, make the quasiparticle approximation in which the spectral weight in MBPT is assumed to be dominated by the quasiparticle peaks, i.e. the properties of the system emerge from the quasiparticle wavefunctions and energies in a similar way to KSDFT, with the important difference that the quasiparticles feel the non-local self-energy operator rather than the exchange-correlation potential, and the quasiparticle band gap is the correct gap rather than the Kohn-Sham gap. In the presence of an electric field, the polarisation of the electron density is described by the density response function. The same change of electron density is described by the Kohn-Sham electrons, responding to the change in their Kohn-Sham potential, as by the quasiparticles, responding to the change in the actual electrostatic potential (external plus Hartree, since the self-energy operator has no long-range part in conventional MBPT). However, in one-electron perturbation theory, the degree of polarisation is inversely proportional to the energy gap, which is smaller in DFT than in quasiparticle theory. To compensate, the strength of the long-range part of the Kohn-Sham potential must be weaker; this is achieved by the xc field. Godby and Sham, making the further approximation that the quasiparticle wavefunctions were similar to the Kohn-Sham wavefunctions, deduced that

$$\frac{\Delta V_{xc}}{\Delta V} \approx -\frac{\Delta_{xc}}{E_{gap}} \; , \tag{5.21}$$

where ΔV_{xc} is the strength of the xc field, ΔV is the strength of the actual electrostatic field, and E_{gap} is the quasiparticle band gap. This fraction is significant: about -0.5 in silicon, for instance.

In reciprocal space, Ghosez *et al.* [67] showed that the xc field corresponds to a $1/q^2$ divergence in the exchange-correlation kernel for small wavevectors q. This ultra-non-local density dependence is certainly missing from all density based approximations to the exact xc functional, potential or kernel. One possibility for approximating it within Kohn-Sham DFT has been explored recently by de Boeij *et al.* [68] by using a functional of the current rather than the density, in the low-frequency limit of time-dependent DFT.

---

[8] That is, mathematically non-local but with the range of the non-locality restricted to a few ångstroms.

5.4 Total Energies from Many-Body Theory

To apply the KS method to real problems with confidence in its predictive accuracy, we need reasonable approximations to the exchange-correlation energy functional. However, we have seen in the previous section that $E_{\mathrm{xc}}[n]$ is a very peculiar object which is described far from properly by the common local-density or generalised gradient approximations. Thus, although the basic reason for the success of the LDA was understood many years ago [42,69], there are a number of well identified cases in which LDAs and GGAs fail dramatically. For instance, they give qualitatively wrong structural results when studying not only some strongly correlated materials [70], but also in some systems dominated by sp bonds [71,72]; or they systematically overestimate cohesive energies and underestimate the activation barrier of chemical reactions [73]. This is not a surprise because, in essence, LDA/GGAs are limited by their intrinsic semi-local nature and by the absence of self-interaction corrections.

To some extent, all the acknowledged improvements upon LDA/GGAs start from model systems (usually the homogeneous electron gas). It would be desirable for a total energy method not to rely on the similarity of a system to a particular reference, thus having a truly *ab-initio* technique. Configuration interaction (CI) and quantum Monte Carlo (QMC) [74] are examples of such methods. Both procedures are in principle exact, but the scaling of CI with system size implies an almost prohibitive computational effort even in medium-size problems. QMC calculations are less demanding, but they are still much more expensive than standard DFT.

MBPT-based schemes can be meant as an alternative for those situations in which known DFT models are inaccurate, but whose complexity makes the implementation of QMC difficult. In this section, after a brief summary of the theoretical foundations, we will review some of the recent applications which, so far, have been restricted to model systems but in which LDA/GGAs clearly show their limitations. Finally, we will present a simplified many-body theory amenable for its implementation in a DFT-fashion.

5.4.1 Theoretical Background

Although many-body theory gives *per se* enough information to obtain the ground-state energy $E^{(0)}$ of an electron system, it is useful to keep a link between MBPT- and DFT-based expressions. First, it is computationally more convenient to evaluate the *difference* between MBPT and KS results than the full energy given by MBPT. Second, a fully self-consistent calculation can be achieved in the framework of MBPT, but a first estimation of the results beyond LDA can be obtained just by evaluating the many-body corrections over the LDA-KS system, using the KS system as a zeroth-order approximation – as it is done, for instance, in the G_0W_0 method. It is convenient,

on occasion, to write down many-body-based expressions for the xc energy, defined precisely as in exact KS-DFT.

MBPT provides several ways to obtain each of the different contributions to the ground-state energy $E^{(0)}$. Perhaps the best known, owing to its role in the construction of xc energy functionals, is the expression based on the adiabatic-connection-fluctuation-dissipation (ACFD) theorem [75,76]

$$
E_{\mathrm{xc}}\left[n_0\right] = \frac{1}{2} \int_0^1 \mathrm{d}\lambda \int \mathrm{d}\boldsymbol{r}\,\mathrm{d}\boldsymbol{r}' \frac{1}{|\boldsymbol{r}-\boldsymbol{r}'|} \tag{5.22}
$$
$$
\times \left[n_0\left(\boldsymbol{r}\right)\delta\left(\boldsymbol{r}-\boldsymbol{r}'\right) - \int_0^{+\infty}\frac{\mathrm{d}\omega}{\pi}\chi_\lambda\left(\boldsymbol{r},\boldsymbol{r}';\mathrm{i}\omega\right) \right] \ .
$$

Here, $\chi_\lambda\left(\mathrm{i}\omega\right)$ is the causal density response function at imaginary frequencies of a system in which the electrons interact through a modified Coulomb potential $w_\lambda\left(r\right) = \lambda/r$, and whose ground state density is equal to the actual one. $\chi_\lambda\left(\mathrm{i}\omega\right)$ is related to the polarisation function $P_\lambda\left(\mathrm{i}\omega\right)$ through the equality[9]

$$
\widehat{\chi}_\lambda\left(\mathrm{i}\omega\right) = \widehat{P}_\lambda\left(\mathrm{i}\omega\right)\left[1 - \widehat{w}_\lambda \widehat{P}_\lambda\left(\mathrm{i}\omega\right)\right]^{-1}\ , \tag{5.23}
$$

where usual matrix multiplications are implied. For practical purposes, we subtract from (5.22) the exact exchange energy functional

$$
E_{\mathrm{x}}\left[n_0\right] = -\sum_\sigma \int \mathrm{d}\boldsymbol{r}\,\mathrm{d}\boldsymbol{r}' \frac{\left|\sum_j^{\mathrm{occ}}\phi_j^*\left(\boldsymbol{r},\sigma\right)\phi_j^*\left(\boldsymbol{r}',\sigma\right)\right|^2}{2\left|\boldsymbol{r}-\boldsymbol{r}'\right|} = \tag{5.24}
$$
$$
= \int \mathrm{d}\boldsymbol{r}\,\mathrm{d}\boldsymbol{r}' \frac{1}{2\left|\boldsymbol{r}-\boldsymbol{r}'\right|}\left[n_0\left(\boldsymbol{r}\right)\delta\left(\boldsymbol{r}-\boldsymbol{r}'\right) - \int_0^{+\infty}\frac{\mathrm{d}\omega}{\pi}\chi_0\left(\boldsymbol{r},\boldsymbol{r}';\mathrm{i}\omega\right) \right]\ ,
$$

where $\chi_0\left(\mathrm{i}\omega\right) \equiv P_{\mathrm{KS}}\left(\mathrm{i}\omega\right)$ is the density response of the fictitious KS system

$$
\widehat{\chi}_0\left(\boldsymbol{r},\boldsymbol{r}';\mathrm{i}\omega\right) = \sum_\sigma \sum_{i,j} \frac{\left(f_i - f_j\right)\phi_i^*\left(\boldsymbol{r},\sigma\right)\phi_i\left(\boldsymbol{r}',\sigma\right)\phi_j\left(\boldsymbol{r},\sigma\right)\phi_j^*\left(\boldsymbol{r}',\sigma\right)}{\varepsilon_i^{\mathrm{KS}} - \varepsilon_j^{\mathrm{KS}} + \mathrm{i}\omega}\ ,
$$
$$
\tag{5.25}
$$

f_j being the Fermi occupation (0 or 1) of the j-th KS orbital. As a consequence, the correlation energy can be evaluated as

$$
E_{\mathrm{c}}\left[n_0\right] = \int_0^1 \mathrm{d}\lambda\, \mathrm{tr}\left\{ \widehat{w}\int_0^{+\infty}\frac{\mathrm{d}\omega}{2\pi}\left[\widehat{\chi}_0\left(\mathrm{i}\omega\right) - \widehat{\chi}_\lambda\left(\mathrm{i}\omega\right)\right] \right\}\ , \tag{5.26}
$$

where "tr" stands for the spatial trace. Note that if we set $P_\lambda \simeq P_{\mathrm{KS}}$ in (5.23) we have the random phase approximation (RPA) – strictly speaking, an LDA-based RPA since the local density is used to obtain the one-electron orbitals and energies.

---

[9] We can establish this relation because at imaginary frequencies the causal and the time-ordered response functions coincide.

The same information can be also extracted from the self-energy operator and the Green's function. Namely, using the adiabatic-connection that led to (5.22)[10]

$$E_{xc}[n_0] = -\frac{i}{2} \int_0^1 \frac{d\lambda}{\lambda} \int_{-\infty}^{+\infty} \frac{d\omega}{2\pi} \int d\boldsymbol{x}\, d\boldsymbol{x}' \, \Sigma_\lambda(\boldsymbol{x}, \boldsymbol{x}'; \omega)\, G_\lambda(\boldsymbol{x}', \boldsymbol{x}; \omega) \ , \quad (5.27)$$

where, again, Σ_λ and G_λ refer to a fictitious system with the scaled Coulomb potential w_λ, and a convergence factor $\exp(i\eta\omega)$ is to be understood in the ω integral. Nonetheless, the one-electron density matrix $\gamma(\boldsymbol{x}, \boldsymbol{x}')$ can be obtained directly from G:

$$\gamma(\boldsymbol{x}, \boldsymbol{x}') = -i \int \frac{d\omega}{2\pi} G(\boldsymbol{x}, \boldsymbol{x}'; \omega) \ , \quad (5.28)$$

and the Green's function provides the expectation value of any one-particle operator[11]. Thus, it is more convenient to calculate explicitly the kinetic energy contribution to E_{xc} rather than making the adiabatic connection:

$$E_{xc}[n_0] = -\frac{i}{2} \int_{-\infty}^{+\infty} \frac{d\omega}{2\pi} \int d\boldsymbol{x}\, d\boldsymbol{x}' \, \Sigma(\boldsymbol{x}, \boldsymbol{x}'; \omega)\, G(\boldsymbol{x}', \boldsymbol{x}; \omega)$$
$$-i \int_{-\infty}^{+\infty} \frac{d\omega}{2\pi} \int d\boldsymbol{x} \lim_{\boldsymbol{x}' \to \boldsymbol{x}} \left[-\frac{\nabla^2}{2} \delta G(\boldsymbol{x}, \boldsymbol{x}'; \omega) \right] \ , \quad (5.29)$$

where $\delta G = G - G_{KS}$ is the difference between the Green's function of the real system and the KS one. Finally, if we separate the exchange and correlation contributions to (5.29) using

$$E_x[n_0] = -\frac{i}{2} \int_{-\infty}^{+\infty} \int d\boldsymbol{x}\, d\boldsymbol{x}' \, \frac{d\omega}{2\pi} \Sigma_x(\boldsymbol{x}, \boldsymbol{x}')\, G_{KS}(\boldsymbol{x}', \boldsymbol{x}; \omega) \ , \quad (5.30)$$

[10] As shown in [75,76], the xc energy of an electron system can be written as:

$$E_{xc}[n_0] = \int_0^1 \frac{d\lambda}{\lambda} \left(\left\langle \widehat{W} \right\rangle_\lambda - E[\lambda, n_0] \right) = \int_0^1 \frac{d\lambda}{\lambda} W_{xc}[\lambda, n_0]$$

Here, $\left\langle \widehat{W} \right\rangle_\lambda$ is the expectation value of the electron-electron interaction energy of the fictitious system whose ground-state density is n_0 but interacting through the potential λ/r, and $E[\lambda, n_0] = \lambda E[n_0]$ is the corresponding Hartree classical contribution. If we evaluate W_{xc} in terms of the density response function of the fictitious system we arrive at (5.22). By using the self-energy and the Green's function instead, we get the expression (5.27).

[11] For instance, the electron density is simply given by

$$n(\boldsymbol{r}) = -i \sum_\sigma \int \frac{d\omega}{2\pi} G(\boldsymbol{x}, \boldsymbol{x}; \omega)$$

As a consequence, we might also calculate the MBPT corrections to the LDA/GGA density for those systems in which they are expected to be inaccurate and, hence, to the classical Hartree electrostatic energy.

with Σ_x the Fock operator of the KS system

$$\Sigma_{\mathrm{x}}\left(\boldsymbol{x},\boldsymbol{x}\right)=-\sum_{i}^{\mathrm{occ}}\frac{\phi_{i}\left(\boldsymbol{x}\right)\phi_{i}^{*}\left(\boldsymbol{x}'\right)}{\left|\boldsymbol{r}-\boldsymbol{r}'\right|}\ ,\tag{5.31}$$

we arrive at the definite expression

$$E_{\mathrm{c}}\left[n_{0}\right]=-\mathrm{i}\int_{-\infty}^{+\infty}\frac{\mathrm{d}\omega}{2\pi}\,\mathrm{Tr}\left[\frac{1}{2}\widehat{\Sigma}_{\mathrm{c}}\left(\omega\right)\widehat{G}\left(\omega\right)+\left(\frac{1}{2}\widehat{\Sigma}_{\mathrm{x}}+\widehat{t}\right)\delta\widehat{G}\left(\omega\right)\right]\tag{5.32}$$

$$=\int_{0}^{+\infty}\frac{\mathrm{d}\omega}{\pi}\,\mathrm{Tr}\left[\frac{1}{2}\widehat{\Sigma}_{\mathrm{c}}\left(\mu+\mathrm{i}\omega\right)\widehat{G}\left(\mu+\mathrm{i}\omega\right)+\left(\frac{1}{2}\widehat{\Sigma}_{\mathrm{x}}+\widehat{t}\right)\delta\widehat{G}\left(\mu+\mathrm{i}\omega\right)\right]\ ,$$

where we have deformed the contour to the imaginary axis. In (5.32), "Tr" is the total trace – including the spin, in contrast to "tr" in (5.26), $\Sigma_{\mathrm{c}} = \Sigma - \Sigma_{\mathrm{x}}$ is the correlation part of the self-energy, and $\widehat{t}$ is the one-particle kinetic energy operator. It is also worth noting that the whole ground-state energy can be written just in terms of the Green's function using the so-called Galitskii-Migdal formula [77]

$$E^{(0)}=\frac{1}{2}\int_{-\infty}^{\mu}\mathrm{d}\omega\,\mathrm{Tr}\left[\left(\omega+\widehat{h}_{0}\right)\widehat{A}\left(\omega\right)\right]\ ,\tag{5.33}$$

with $\widehat{A}\left(\omega\right)$ the spectral function and $\widehat{h}_{0}=\widehat{t}+\widehat{v}_{\mathrm{ion}}$, which, after the inclusion of the remaining contributions to the energy, is equivalent to (5.32). Finally, although we do not discuss them in detail, we have to mention that the ground-state energy can be also obtained from the many-body Luttinger-Ward variational functional [78] and extensions thereof like the Almbladh-von Barth-van Leeuwen theory [79], which are closely related to the Green's function-based formulation we have described here.

It is evident that if the exact theory were used, all the quoted methods would give the same result. Nonetheless, in practical implementations we have to resort to further approximations. The ACFD expression (5.26) requires the knowledge of the interacting response function χ_{λ}, which is a quantity that can be obtained in the framework of time-dependent DFT [80,81]. Galitskii-Migdal and Luttinger-Ward-like methods need the interacting many-body Green's function[12]. We shall focus mainly on Green's-function-based evaluations – e.g. equations (5.32) and (5.33) – of the ground-state properties, but we note that several ACFD approaches have been used to study the HEG [82], the van der Waals interaction between two thin metal slabs [83], the jellium surface energy [84], and molecular properties like atomisation energies, bond lengths, and dissociation curves [85,86]. Many-body variational functionals have not been so widely tested, and applications to electron systems have been restricted to the HEG [87], closed-shell atoms [88], and the hydrogen molecule [89].

---

[12] Because of the close relation between P and χ, the response function may be also obtained from many-body approaches.

Table 5.2. Correlation energy per particle (in Ha) for the spin-unpolarised phase of the 3D electron gas obtained using several GW schemes, QMC, and RPA. For reference, the exchange energy per particle is included in the last row

r_s	1	2	4	5	10
QMC[a]	−0.060	−0.045	−0.032	−0.028	−0.019
QMC[b]	−0.055	−0.042		−0.028	
GW[c]	−0.058	−0.044	−0.031	−0.027	−0.017
GW[d]		−0.045	−0.032		
GW_0[c]	−0.061	−0.043	−0.028	−0.024	−0.015
G_0W_0[c]	−0.070	−0.053	−0.038	−0.033	−0.021
RPA	−0.079	−0.062	−0.047	−0.042	−0.031
ε_x	−0.458	−0.229	−0.115	−0.092	−0.046

[a] Reference [94]
[b] Reference [95]
[c] Reference [92]
[d] Reference [91]

5.4.2   Applications

The first application of Green's function theory to the calculation of ground-state properties of the three-dimensional (3D) homogeneous electron gas (HEG) at metallic densities appeared in a seminal work by Lundqvist and Samathiyakanit in the late 1960s [90]. However, systematic studies on the performance of Hedin's GW method for the same model were published only a few years ago by von Barth and Holm [37,91], and extended by García-González and Godby [92] to the spin-polarised 3D HEG, and the 2D HEG (a system where GW might be expected to perform less well because correlation is stronger).

   As we may see in Table 5.2, the non-self-consistent G_0W_0 underestimates the total energy of the spin-unpolarised 3D HEG at metallic densities around 10 mHa per electron, which is half the error in the ACFD-RPA [93]. The same trend – that is, a 50% reduction of the RPA error – also appears in the spin-polarised 3D electron gas. A better performance is achieved by using the partially self-consistent GW_0 and, strikingly, at full self-consistency there is an almost perfect agreement with the exact QMC data [94,95]. Moreover, at lower densities and at the 2D HEG – where, as commented, the diagrams not included in GW are more relevant – the GW greatly improves the RPA energies. Thus, we may conclude that *the greater the self-consistency the more accurate the total-energy results*, in marked contrast with the tendency described in Sect. 5.2 for the QP energy dispersion relation.

   The accuracy of GW may be traced back to the fulfilment of all conservation rules in the framework of the theory developed by Baym and
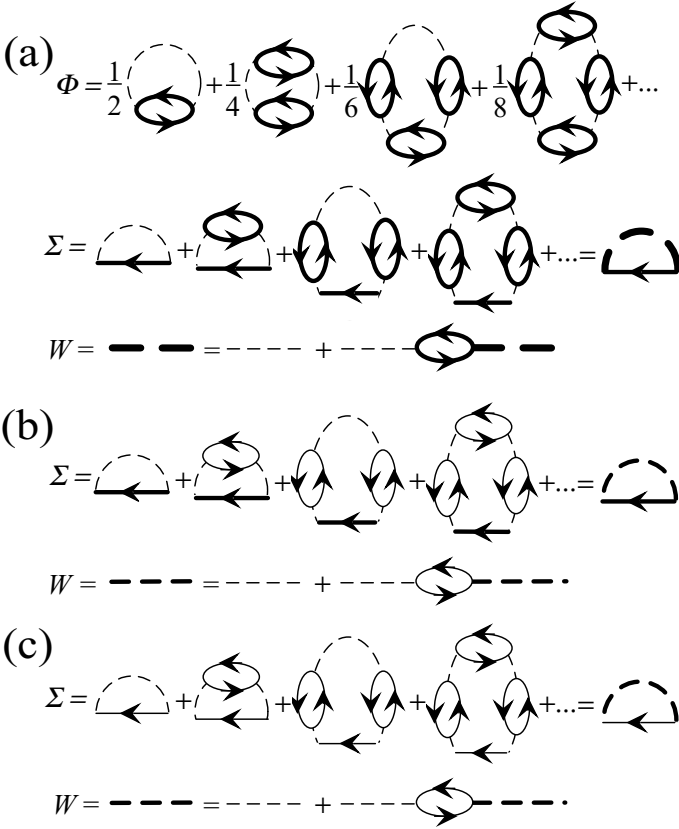
Fig. 5.7. Diagrammatic representation of the self-energy and the screened Coulomb potential in (**a**) the fully self-consistent GW approximation, (**b**) the partially self-consistent GW_0 approximation, and (**c**) the G_0W_0 approximation. The generating functional Φ is also represented in (**a**)

Kadanoff [96]. As showed by Baym [97], the self-energy operator of a conserving approach can be represented as the derivative of a generating functional Φ:

$$\widehat{\Sigma} = \frac{\delta}{\delta \widehat{G}} \Phi\left[\widehat{G}\right] , \tag{5.34}$$

which has to be evaluated self-consistently at the Green's function that is the solution of the Dyson equation (5.10e). The self-consistent GW approximation does derive from a functional Φ_{GW} (see Fig. 5.7). Therefore, its implementation guarantees among other things, the conservation of the number of particles of the system[13]; the coincidence of the Fermi levels obtained by

---

[13] Since we can include the interaction between the electrons in a perturbative fashion, conservation means that GW gives the *correct* number of particles after integration of the corresponding Green's function.

solving the QP equation and by subtracting the ground-state energies of the
N- and $(N-1)$- particle systems; and the equivalence of (5.22) and (5.27)
when calculating xc energies.

Nonetheless, the success of GW when obtaining the ground-state energy
of homogeneous systems has to be taken with caution. First, GW is not so
accurate in highly correlated systems described by simple Hubbard Hamil-
tonians [98,99,100,89], and the GW correlation function of the HEG does
not improve significantly on the RPA [101]. The GW polarisation function
– and, hence, the density response – shows certain unphysical features. It it
also worth noting that, even using the space-time procedure [17][14], a fully
self-consistent resolution of Hedin's GW equations is very demanding for any
inhomogeneous system. As a consequence, efforts to evaluate structural prop-
erties from MBPT should be directed towards non- or partially self-consistent
schemes with further inclusion of short-ranged correlations that are absent
in the GW diagrams. However, there is no guarantee that approximations
other than self-consistent Φ-derivable schemes are conserving theories, and
the fulfillment of exact sum rules by these models should be assessed care-
fully if they are intended to be used as practical tools to evaluate ground-state
properties.

The most fundamental sum rule is the conservation of the number of
particles which is satisfied by the partially self-consistent GW_0 method [102],
even though it is not Φ-derivable. However, as demonstrated by Schindlmayr
in a Hubbard model system [103], G_0W_0 does *not* yield the correct number of
particles. This failure was confirmed by Rieger and Godby for bulk Si [104],
where G_0W_0 slightly underestimates the total number of valence electrons.
A study of particle-number violation in diagrammatic self-energy models has
been recently presented by Schindlmayr *et al.* [105]. These authors provided
a general criterion that allows, by simple inspection, to verify whether an
approximation satisfies the particle-number sum rule. They also showed that
the G_0W_0 particle-number violation is not, in practice, significant within the
range of densities of physical interest (see Fig. 5.8). The same conclusion
applies to models built by insertion of local vertex corrections into a G_0W_0
scheme [25].

The first evidence of the usefulness of these non-self-consistent diagram-
matic schemes to evaluate structural properties has been the application of
G_0W_0 to calculate the ground-state energy of confined quasi-2D systems and
the interaction energy between two thin metal slabs [106]. For the quasi-2D
gas, the high inhomogeneity of the density profile along the confining direc-
tion is clearly beyond the scope of local and semi-local KS-DFT approaches
which, in fact, diverge when approaching the 2D limit [107,108,109]. RPA-
ACFD does not show such a divergence but clearly underestimates the energy
of quasi-2D systems. G_0W_0, whose superiority to the RPA in the 2D and 3D

---

[14] Note that we just need the self-energy and the Green's function at imaginary
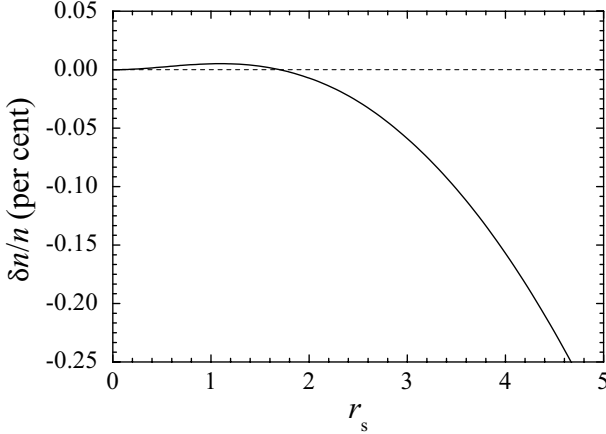frequencies to obtain ground-state properties from MBPT.

Fig. 5.8. Violation of the particle-number sum rule for the homogeneous electron gas in the G_0W_0 approximation. The relative error in the density is always negative and of the order of 0.1% in the range of metallic densities. After Schindlmayr *et al.* [105]

HEG has been already noted, retains this superiority for these quasi-2D systems. Of more direct significance is the study of the interaction between two unconfined jellium slabs. At small distance separation d the density profiles of each subsystem overlap, so having a *covalent bond*. If $d \gg 0$, there is no such overlap and the only source of bonding is the appearance of correlation van der Waals forces which cannot be described at all by KS-LDA/GGA [110]. The xc energy per particle $\varepsilon_{\mathrm{xc}}$ as a function of d is depicted in the upper panel of Fig. 5.9 using the LDA, the RPA, and the G_0W_0, for two slabs of width $L = 12a_0$ and a background density corresponding to $r_{\mathrm{s}} = 3.93$ – the mean density of sodium. In the lower panel, we present the correlation binding energy per particle, defined as $e_{\mathrm{c}}(d) = \varepsilon_{\mathrm{c}}(d) - \varepsilon_{\mathrm{c}}(\infty)$, for the same system. We may see that the local density is unable to reproduce the characteristic asymptotic d^{-2} van der Waals behaviour[15] which, on the contrary, is present in the RPA and G_0W_0 calculations. The results from the two latter approaches are very similar at large separations, which is not a surprise because van der Waals forces are already contained at the RPA level [83]. For intermediate and small separations there are slight differences between RPA and G_0W_0, but much less important than those appearing when comparing the total correlation energies.

It is worth pointing out that the remaining error in the absolute G_0W_0 correlation energy is amenable to an LDA-like correction

$$\Delta E_{\mathrm{c}}[n] = \int \mathrm{d}\boldsymbol{r}\, n(\boldsymbol{r})\, \Delta\varepsilon_{\mathrm{c}}^{GW}(n(\boldsymbol{r}))\ , \tag{5.35}$$

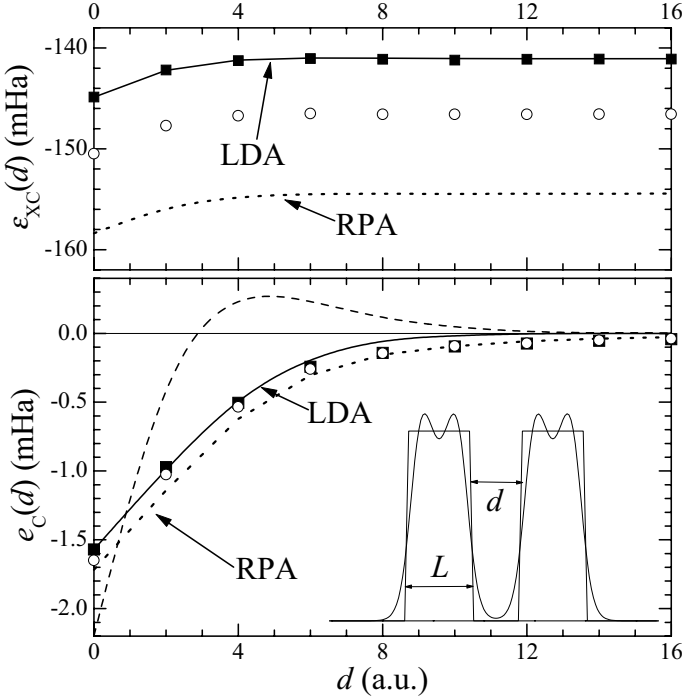[15] Non-local xc functionals such as the ADA or WDA also fail to describe van der Waals forces.

Fig. 5.9. Upper panel: xc energy per particle for two jellium slabs as a function of the distance d (see inset). Lines: LDA and RPA; empty circles: G_0W_0; squares: $G_0W_0+\Delta$. Lower panel: Correlation binding energy per particle. The exchange-only binding energy (dashed line) has been also included in this panel

with[16]

$$\Delta\varepsilon_{\mathrm{c}}^{GW}\left(r_{\mathrm{s}}\right) = \frac{0.04054}{1 + 2.086\sqrt{r_{\mathrm{s}}} + 0.1209r_{\mathrm{s}}^2}\ \mathrm{hartree}\,. \qquad (5.36)$$

Thus, we have a *hybrid* approximation in the spirit of that proposed by Kurth and Perdew [111] for the RPA-ACFD with the further advantage that G_0W_0 and RPA require similar computational effort but $\Delta\varepsilon_{\mathrm{c}}^{GW}\left(r_{\mathrm{s}}\right) < \Delta\varepsilon_{\mathrm{c}}^{\mathrm{RPA}}\left(r_{\mathrm{s}}\right)$. As we can see in Fig. 5.9, the absolute xc energy obtained in this way (which we label as $G_0W_0+\Delta$) is in broad correspondence with the LDA energy, but the binding energy is slightly altered, and, of course, the van der Waals bonding is present. Although, as commented above, these corrections should be described through the implementation of vertex diagrams, this is a first step towards the inclusion of short-ranged correlations.

---

[16] This parameterisation has been obtained by comparing the G_0W_0 and QMC correlation energies in the range $r_{\mathrm{s}} \in [1, 20]$.

5.4.3 Generalised KS Schemes and Self-energy Models

We have seen that many-body-based methods provide an *ab-initio* way to treat the Coulomb correlation in an N electron system without the expensive cost of QMC calculations. However, they are computationally more demanding than routine LDA-KS calculations and, hence, the feasibility of their application to complex systems is unclear, especially in the context of *ab-initio* molecular dynamics calculations, where many total-energy evaluations are required. As described in Sect. 5.3, the main problem when constructing approximations to $E_{xc}[n]$ is related to its inherent non-analytical character which is due to the specific way in which the KS mapping between the real and the fictitious systems is done. However, this *is not* the only possible realisation of DFT and recently, new DFT methods have been proposed [112,113]. In these *generalised* Kohn-Sham schemes (GKS) the actual electron system is mapped onto a fictitious one in which particles move in an effective *non-local* potential. As a result of this, it is possible to describe structural properties at the same (or better) level than LDA/GGA but improving on its description of quasiparticle properties.

Specifically, as shown in [63,64,65], pathologies of the exact KS functional such as the band-gap discontinuity and the xc field may be understood as arising when one transforms a MBPT description, with a non-pathological but non-local self-energy operator, into the KS system with its local potential. In this sense, a non-local xc potential should be more amenable to accurate approximation as an explicit functional of the density.

The GKS approximation proposed by Sánchez-Friera and Godby [114] relies on the use of a jellium-like self-energy to describe the xc effects of inhomogeneous systems:

$$\Sigma^0\left(\boldsymbol{r}, \boldsymbol{r}'; \omega\right) = \frac{v_{xc}^{LDA}\left(\boldsymbol{r}\right) + v_{xc}^{LDA}\left(\boldsymbol{r}'\right)}{2} g\left(\left|\boldsymbol{r} - \boldsymbol{r}'\right|; n_0\right) , \qquad (5.37)$$

where $g(r, n)$ is a parameterised spreading function and n_0 is the mean density of the system. This approximation is suggested by the fact that the frequency-dependence of the self-energy is weak for occupied states, and that for several semiconductors Σ has been shown to be almost spherical and to have the same range than the self-energy of a jellium system with the same mean density [115]. Since (5.37) is real and static, it defines a fictitious system that in this GKS scheme replaces the standard KS non-interacting one, and whose mass operator (Hartree potential plus self-energy) is

$$M_S\left(\boldsymbol{r}, \boldsymbol{r}'\right) = \int d\boldsymbol{r}'' \, \frac{n\left(\boldsymbol{r}''\right)}{\left|\boldsymbol{r} - \boldsymbol{r}''\right|} \delta\left(\boldsymbol{r} - \boldsymbol{r}'\right) + \Sigma^0\left(\boldsymbol{r}, \boldsymbol{r}'; \omega\right) . \qquad (5.38)$$
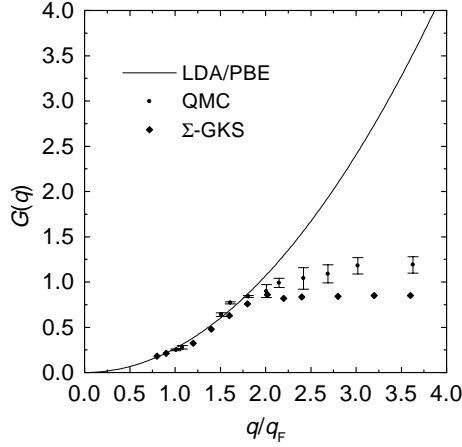
Fig. 5.10. Local field factor $G(q)$ for the linear response of jellium at $r_s = 2$ in the Σ-GKS scheme compared to the QMC results and the LDA/GGA(PBE). After Sánchez-Friera and Godby [114]

The total energy of the actual system is then approximated by

$$E^{(0)} = T_S + \frac{1}{2} \sum_n^{occ} \int d\boldsymbol{r} \, d\boldsymbol{r}' \, \phi_n^*(\boldsymbol{r}) \, M_S(\boldsymbol{r}, \boldsymbol{r}') \, \phi_n(\boldsymbol{r}) \qquad (5.39)$$

$$+ E_{ss}[n] + \int d\boldsymbol{r} \, n(\boldsymbol{r}) \, v_{ion}(\boldsymbol{r}) \ ,$$

where $E_{ss}[n]$ is a local functional that is added so that the model is exact in the homogeneous limit. By minimising (5.39) with respect to variations of the one-particle wavefunctions $\phi_n(\boldsymbol{r})$ a set of self-consistent KS-like equations are obtained. The simple form of the non-locality ensures computational efficiency.

This approximation, labelled as Σ-GKS, shows performance similar to the LDA in the calculation of structural properties of silicon. The most striking feature of this new scheme is the significant improvement when calculating the local field factor of the HEG $G(\boldsymbol{q})$ with respect to local and semi-local approaches. As it is depicted in Fig. 5.10, Σ-GKS fits very well the QMC data by Moroni *et al.* [116] also at large values of the wavevector, where the LDA and the GGA by Perdew, Burke, and Ernzerhof (PBE) [117] fail badly. These results, as well as the efficiency of this new GKS scheme, opens the prospect of a new class of methods that yield accurate total energies and realistic QP spectra through avoiding the pathological aspects of the Kohn-Sham xc energy functional, while retaining computational efficiency comparable to Kohn-Sham DFT.

5.5   Concluding Remarks

In this chapter we have contrasted two approaches to the many-body problem. In Kohn-Sham DFT, fictitious non-interacting electrons move in an effective potential, part of which – the exchange-correlation potential – arises from a functional that in its exact form exhibits complex and sometimes pathological dependence on the electron density, but that in practice is generally approximated by an explicit functional of the density which fails to describe these pathologies. In many-body perturbation theory, electrons move in a spatially non-local, energy-dependent potential which arises from a perturbation expansion which may be evaluated to a chosen order. The calculations are more expensive because of the non-locality and energy-dependence of the self-energy operator, and the need to evaluate a complex expression to obtain it, but the pathologies of the Kohn-Sham functional have no counterparts in MBPT.

We have shown how each theory may be used to illuminate and develop the other. MBPT may be used to exhibit and explore the pathologies of Kohn-Sham DFT with the aim of appreciating the physical effects that are incorrectly described by a given approximate density based functional, and identifying prospects for addressing them in other ways (such as with the explicit wavefunction-dependence of exact-exchange KS-DFT, or current-based functionals). On the other hand, the technology of *ab-initio* DFT calculations has been adapted for MBPT, both for the calculation of quasiparticle and other spectral properties, and, more recently, for ground-state total energy calculations. Also, we have described the possibility of methods intermediate between KS-DFT and MBPT, generalised Kohn-Sham density functional theories, in which the computational efficiency of a density based functional is combined with the physically important non-locality of the self-energy operator.

References

1. P. Hohenberg and W. Kohn, Phys. Rev. **136**, B864 (1964).
2. W. Kohn and L. Sham, Phys. Rev. **140**, A1133 (1965).
3. P. Nozieres, *Theory of Interacting Fermi Systems* (Benjamin, New York, 1964).
4. L. Hedin and S. Lundqvist, in *Solid State Physics*, edited by H. Ehrenreich, F. Seitz, and D. Turnbull (Academic Press, New York, 1969), Vol. 23, p. 1.
5. A. L. Fetter and J. D. Walecka, *Quantum Theory of Many-Particle Systems,* (McGraw-Hill, New York, 1971).
6. G. D. Mahan, *Many-Particle Physics* (Plenum, New York, 1990)
7. E. K. U. Gross, E. Runge, and O. Heinonen, *Many-Particle Theory* (Adam Hilger, Bristol, 1991).
8. L. Hedin, Phys. Rev. **139**, A796 (1965).
9. F. Aryasetiawan and O. Gunnarsson, Rep. Prog. Phys. **61**, 3 (1998).

10. W. G. Aulbur, L. Jönsson, and J. W. Wilkins, in *Solid State Physics,* edited by H. Ehrenreich (Academic Press, Orlando, 2000), Vol. 54, p 1.
11. P. M. Echenique, J. M. Pitarke, E. Chulkov, and A. Rubio, Chem. Phys. **251**, 1 (2000).
12. P. García-González and R. W. Godby, Comp. Phys. Comm. **137**, 108 (2001).
13. G. Onida, L. Reining, and A. Rubio, Rev. Mod. Phys. **74**, 601 (2002).
14. C.-O. Almbladh and L. Hedin, in *Handbook on Synchrotron Radiation*, edited by E. E. Koch (North-Holland, 1983), Vol 1.
15. D. Pines, *Elementary excitations in solids*(Benjamin, New York, 1964).
16. B. I. Lundqvist, Phys. Kondens. Mater. **6**, 193 (1967). W. von der Linden and P. Horsch, Phys. Rev. B **37**, 8351 (1988). G. E. Engel and B. Farid, Phys. Rev. B **47**, 15931 (1993).
17. H. N. Rojas, R. W. Godby, and R. Needs, Phys. Rev. Lett. **74**, 1827 (1995).
18. M. M. Rieger, L. Steinbeck, I. D. White, N. H. Rojas, and R. W. Godby, Comp. Phys. Comm. **117**, 211 (1999); L. Steinbeck, A. Rubio, L. Reining, M. Torrent, I. D. White, and R. W. Godby, *ibid* **125**, 105 (2000).
19. M. S. Hybertsen and S. G. Louie, Phys. Rev. Lett. **55**, 1418 (1985).
20. S. Saito, S. B. Zhang, S. G. Louie, and M. L. Cohen, Phys. Rev. B **40**, 3643 (1989).
21. G. Onida, L. Reining, R. W. Godby, R. Del Sole, and W. Andreoni, Phys. Rev. Lett. **75**, 818 (1995).
22. P. Rinke, P. García-González, and R. W. Godby (unpublished).
23. R. Del Sole, L. Reining, and R. W. Godby, Phys. Rev. B **49**, 8024 (1994).
24. M. Hindgren and C.-O. Almbladh, Phys. Rev. B **56**, 12832 (1997).
25. P. García-González and R. W. Godby (unpublished).
26. D. Langreth, Phys. Rev. B **1**, 471 (1970).
27. F. Aryasetiawan, L. Hedin, and K. Karlsson, Phys. Rev. Lett. **77**, 2268 (1996).
28. E. Jensen and E. W. Plummer, Phys. Rev. Lett. **55**, 1912 (1985).
29. B. S. Itchkawitz, I.-W. Lyo, and E. W. Plummer, Phys. Rev. B **41**, 8075 (1990).
30. J. E. Northrup, M. S. Hybertsen, and S. G. Louie, Phys. Rev. Lett. **59**, 819 (1989).
31. W.-D. Schöne and A. G. Eguiluz, Phys. Rev. Lett. **81**, 1662 (1998).
32. G. D. Mahan and B. E. Sernelius, Phys. Rev. Lett. **62** 2718 (1989).
33. H. Yasuhara, S. Yoshinaga, and M. Higuchi, Phys. Rev. Lett. **83**, 3250 (1999).
34. K. W.-K. Shung and G. D. Mahan, Phys. Rev. B **38**, 3856 (1988).
35. Y. Takada, Phys. Rev. Lett. **87**, 226402 (2001).
36. U. von Barth and B. Holm, Phys. Rev. B **54**, 8411 (1996).
37. B. Holm and U. von Barth, Phys. Rev. B **57**, 2108 (1998).
38. N. Hamada, M. Hwang, and A. J. Freeman, Phys. Rev. B **41**, 3620 (1990).
39. B. Arnaud and M. Alouani, Phys. Rev. B 562, 4464 (2000).
40. W. Ku and A. G. Eguiluz, Phys. Rev. Lett. **89**, 126401 (2002).
41. P. A. Bobbert and W. van Haeringen, Phys. Rev. B **49**, 10326 (1994).
42. O. Gunnarsson, M. Jonson, and B. I. Lundqvist, Phys. Rev. B **20**, 3136 (1979).
43. E. Chacón and P. Tarazona, Phys. Rev. B **37**, 4013 (1988).
44. J. A. Alonso and N. A. Cordero, in *Recent Developments and Applications of Modern Density Functional Theory*, edited by J. M. Seminario (Elsevier, Amsterdam, 1996) and references therein.
45. J. D. Talman and W. F. Shadwich, Phys. Rev. A **14**, 36 (1976).

46. V. Sahni, J. Gruenebaum, and J. P. Perdew, Phys. Rev. B **26**, 4371 (1982).
47. J. P. Perdew and M. Levy, Phys. Rev. Lett. **51**,1881 (1983).
48. L. J. Sham and M. Schlüter, Phys. Rev. Lett. **51**, 1888 (1983).
49. R. G. Parr and W. Yang, *Density Functional Theory of Atoms and Molecules* (Oxford University Press, New York, 1989).
50. R. M. Dreizler and E. K. U. Gross, *Density Functional Theory: An Approach to the Quantum Many-Body Problem* (Springer-Verlag, Berlin, 1990).
51. C.-O. Almbladh and U. von Barth, Phys. Rev. B **31**, 3231 (1985).
52. R. W. Godby, L. J. Sham, and M. Schlüter, Phys. Rev. Lett. **56**, 2415 (1986).
53. R. W. Godby, L. J. Sham, and M. Schlüter, Phys. Rev. B **36**, 6497 (1987).
54. L. J. Sham and M. Schlüter, Phys. Rev. B **32**, 3883 (1985).
55. W. Knorr and R. W. Godby, Phys. Rev. Lett. **65**, 639 (1992); Phys. Rev. B **50**, 1779 (1994).
56. O. Gunnarsson and K. Schönhammer, Phys. Rev. Lett. **56**, 1968 (1986).
57. M. Städele, M. Mouraka, J. A. Majewski, P. Vogl, and A. Görling, Phys. Rev. B **59**, 10031 (1999).
58. W. G. Aulbur, M. Städele, and A. Görling, Phys. Rev. B **62**, 7121 (2000).
59. A. Görling and M. Levy, Phys. Rev. A **52**, 4493 (1995); A. Görling, *ibid.* **54**, 3912 (1996).
60. C.-O. Almbladh and U. von Barth, in *Density Functional Methods in Physics*, edited by R. M. Dreizler and J. da Providência (Plenum Press, New York, 1985), p. 209.
61. J. Katriel and E. R. Davidson, Proc. Nat. Acad. Sci. USA **77**, 4403 (1980).
62. R.W. Godby, L.J. Sham and M. Schlüter, Phys. Rev. Lett. **65**, 2083 (1990).
63. R.W. Godby and L.J. Sham, Phys. Rev. B **49**, 1849 (1994).
64. X. Gonze, P. Ghosez and R. W. Godby, Phys. Rev. Lett. **74**, 4035 (1995).
65. X. Gonze, P. Ghosez and R. W. Godby, Phys. Rev. Lett. **78**, 294 (1997).
66. X. Gonze, P. Ghosez and R. W. Godby, Phys. Rev. Lett. **78**, 2029 (1997).
67. P. Ghosez, X. Gonze and R. W. Godby, Phys. Rev. B **56**, 12811 (1997).
68. P. L. de Boeij, F. Kootstra, J. A. Berger, R. van Leeuwen, and J. G. Snijders, J. Chem. Phys. 15, 1995 (2001).
69. R. O. Jones and O. Gunnarsson, Rev. Mod. Phys **61**, 689 (1989).
70. H. Sawada and K. Terakura, Phys. Rev. B **58**, 6831 (1998).
71. J. C. Grossman, L. Mitas, and K. Raghavachari, Phys. Rev. Lett. **75**, 3870 (1995).
72. P. R. C. Kent, M. D. Towler, R. J. Needs, and G. Rajagopal, Phys. Rev. B **62**, 15394 (2000).
73. J. C. Grossman and L. Mitas, Phys. Rev. Lett. **79**, 4353 (1997).
74. W. M. C. Foulkes, L. Mitas, R. J. Needs, and G. Rajagopal, Rev. Mod. Phys. **73**, 17 (2000).
75. D. C. Langreth and J. P. Perdew, Solid State Commun. **17**, 1425 (1975); Phys. Rev. B **15**, 2884 (1977).
76. W. Kohn and P. Vashishta, in *Theory of the Inhomogeneous Electron Gas*, edited by S. Lundqvist and N. H. March (Plenum, New York, 1983).
77. V. M. Galitskii and A. B. Migdal, Zh. Éksp. Teor. Fiz. **34**, 139 (1958) [Sov. Phys. JETP **7**, 96 (1958)].
78. J. M. Luttinger and J. C. Ward, Phys. Rev. **118**, 1417 (1960).
79. C.-O. Almbladh, U. von Barth, and R. van Leeuwen, Int. J. Mod. Phys. B **13**, 535 (1999).

80. E. Runge and E. K. U. Gross, Phys. Rev. Lett. **52**, 997 (1984).
81. E. K. U. Gross, C. A. Ullrich, and U. J. Grossman, in *Density Functional Theory*, edited by E. K. U. Gross and R. M. Dreizler (Plenum, New York, 1995).
82. M. Lein, E. K. U. Gross, and J. P. Perdew, Phys. Rev. B **61**, 13431 (2000) and references therein.
83. J. F. Dobson and J. Wang, Phys. Rev. Lett. **82**, 2123 (1999); Phys. Rev. B **62**, 10038 (2000).
84. J. M. Pitarke and A. Eguiluz, Phys. Rev. B **57**, 6329 (1998); **63**, 045116 (2001).
85. F. Furche, Phys. Rev. B **64**, 195120 (2001).
86. M. Fuchs and X. Gonze, Phys. Rev. B **65**, 235109 (2002).
87. M. Hindren, PhD. thesis, Lund University, 1997.
88. N. E. Dahlen and U. von Barth (unpublished).
89. F. Aryasetiawan, T. Mikaye, and K. Terakura, Phys. Rev. Lett. **88**, 166401 (2002).
90. B. I. Lundqvist and V. Samathiyakanit, Phys. Kondens. Mater. **9**, 231 (1969).
91. B. Holm, Phys. Rev. Lett. **83**, 788 (1999).
92. P. García-González and R. W. Godby, Phys. Rev. B **63**, 075112 (2001).
93. R. F. Bishop and K. H. Lührmann, Phys. Rev. B **26**, 5523 (1982).
94. D. M. Ceperley and B. J. Adler, Phys. Rev. Lett. **45**, 566 (1980).
95. G. Ortiz, M. Harris, and P. Ballone, Phys. Rev. Lett. **82**, 5317 (1999); G. Ortiz and P. Ballone, Phys. Rev. B **50**, 1391 (1994).
96. G. Baym and L. P. Kadanoff, Phys. Rev. **124**, 287 (1961).
97. G. Baym, Phys. Rev. **127**, 1391 (1962).
98. C. Verdozzi, R. W. Godby and S. Holloway, Phys. Rev. Lett. **74**, 2327 (1995).
99. A. Schindlmayr, T. J. Pollehn and R. W. Godby, Phys. Rev. B **58** 12684-90 (1998).
100. T. J. Pollehn, A. Schindlmayr and R. W. Godby, J. Phys.: Condens. Matter **10** 1273-1283 (1998).
101. B. Holm and U. von Barth (unpublished).
102. B. Holm, PhD thesis, Lund University (1997).
103. A. Schindlmayr, Phys. Rev. B **56**, 3528 (1997).
104. M. M. Rieger and R. W. Godby, Phys. Rev. B **58**, 1343 (1998).
105. A. Schindlmayr, P. García-González, and R. W. Godby, Phys. Rev. B **64**, 235106 (2001).
106. P. García-González and R. W. Godby, Phys. Rev. Lett. **88**, 056406 (2002).
107. Y.-H. Kim, I.-H. Lee, S. Nagaraja, J.-P. Leburton, R. Q. Hood, and R. M. Martin, Phys. Rev. B **61**, 5202 (2000).
108. L. Pollack and J. P. Perdew, J. Phys.: Condens. Matter **12**, 1239 (2000)
109. P. García-González, Phys. Rev. B **62**, 2321 (2000).
110. W. Kohn, Y. Meir, and D. E. Makarov, Phys. Rev. Lett. **80**, 4153 (1998).
111. S. Kurth and J. P. Perdew, Phys. Rev. B **59**, 10146 (1999).
112. A. Seidl, A. Görling, P. Vogl, J. A. Majewski, and M. Levy, Phys. Rev. B **53**, 3764 (1996).
113. G. E. Engel, Phys. Rev. Lett. **78**, 3515 (1997).
114. P. Sánchez-Friera and R. W. Godby, Phys. Rev. Lett. **85**, 5611 (2000).
115. R. W. Godby, M. Schlüter, and L. J. Sham, Phys. Rev. B **37**, 10159 (1988).
116. S. Moroni, D. M. Ceperley, and G. Senatore, Phys. Rev. Lett. **75**, 689 (1995).
117. J. P. Perdew, K. Burke, and M. Ernzerhof, Phys. Rev. Lett. **77**, 3685 (1996).